

Synthesis and Characterization of Yttrium Iron Garnet Nanoparticles

P. Vaqueiro,* M. P. Crosnier-Lopez,† and M. A. López-Quintela*

*Departamento de Química Física, Facultad de Química, Universidad de Santiago de Compostela, E-15706, Spain; and †Laboratoire des Fluorures, URA CNRS 449, Faculté des Sciences, Université du Maine, 72017 Le Mans, France

Received March 4, 1996; in revised form June 14, 1996; accepted July 1, 1996

Yttrium iron garnet (YIG) was synthesized from a citrate gel containing ethylene glycol. The conditions for obtaining the pure phase depending on the citric acid/ethylene glycol ratio were studied. The sizes of the obtained particles ranged from 20 to 500 nm with the annealing temperature. Particles exhibited a rounded surface morphology, without faceted borders. © 1996

Academic Press, Inc.

INTRODUCTION

Yttrium iron garnet (YIG), a material widely used in microwave devices, is usually prepared by heating a mixture of Y_2O_3 and Fe_2O_3 above $1300^\circ C$ for several hours (1). This process involves extensive treatments at high temperature and repeated mechanical mixing to achieve the desired phase purity. Other techniques for synthesizing garnets using hydroxide coprecipitation (2), hydrolysis of metal alkoxides (3), or decomposition of a citrate gel (4, 5) have been developed. In these methods, the reactant cations are intimately mixed on the atomic scale, so the rate of the reaction will be increased, leading to lower synthesis temperatures and smaller particles.

Garnets have been synthesized by the citrate gel process, but in the literature the conditions of preparation are not well established. In this paper we report a preparation method, as well as the structural and microstructural properties of the prepared samples as a function of the annealing treatment, on the basis of X-ray diffraction and transmission electron microscopy.

EXPERIMENTAL PROCEDURE

A scheme of the preparation method detailed below is shown in Fig. 1. Stoichiometric mixtures of nitrates of iron(III) (Aldrich 98%) and yttrium(III) (Aldrich 99%) were dissolved in an aqueous solution of citric acid (Aldrich, 99%). Ethylene glycol (Fluka, 99.5%) was added and the resulting solution was heated at $80^\circ C$ in order to obtain

the gel. Gels were prepared with different quantities of ethylene glycol (see Table 1), since in the literature it is reported that the presence of ethylene glycol improves the synthesis process (6). Also, the influence of citric acid concentration was studied by preparing gels with different quantities of citric acid. To obtain the YIG samples, gels were dried initially at $110^\circ C$ for 36 h and further heat treated in air at temperatures between 400 and $1000^\circ C$ and for periods of time between 2 and 24 h. The conditions of annealing of the series A samples are listed in Table 2.

X-RAY DIFFRACTION

The samples were characterized by X-ray diffraction using a Philips PW-1710 diffractometer equipped with a Cu anode ($CuK\alpha$ radiation) and a graphite monochromator. The different phases were identified using the JCPDS Powder Diffraction Files (7). Crystallographic data for these phases are given in Table 3.

In Fig. 2, one can observe that samples treated at 400 and $600^\circ C$ are mainly amorphous and that the crystallization process begins at about $700^\circ C$. This crystallization temperature is lower than the $1300^\circ C$ used in the ceramic method and allows small particles to be obtained. XRD patterns recorded from samples of series A to F heated at 800, 900, and $1000^\circ C$ are similar to that of standard YIG, although for the samples prepared with ethylene glycol there is also a peak at $33.2^\circ (2\theta)$ with low intensity ($\sim 1\%$). This could be attributed to a small volume fraction of hematite, $\alpha-Fe_2O_3$, and/or orthoferrite, $YFeO_3$. In the samples of series G, H, and I, larger quantities of orthoferrite and hematite are present (see Fig. 3). Therefore, the addition of ethylene glycol to the initial gel in small quantities (series H and I) leads to the presence of orthoferrite and hematite. With larger quantities of ethylene glycol (series D, E, F, and G), the orthoferrite and hematite percentage decreases, but even in the samples prepared with the largest quantity of ethylene glycol, orthoferrite and hematite are still present.

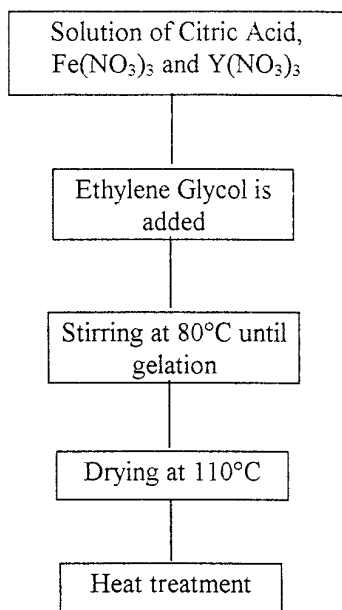


FIG. 1. Schematic representation of the synthesis process.

In the case of the samples heated at 400 and 600°C, the structure of XRD patterns results from two contributions: a broad band of high intensity and broad peaks of low intensity. These peaks can be attributed to magnetite (Fe_3O_4) or maghemite ($\gamma\text{-Fe}_2\text{O}_3$) and the broad band to an amorphous garnet phase. The contribution of the first phase is greater when the samples are prepared with ethylene glycol, and this contribution decreases with larger quantities of citric acid.

The patterns of the samples heated at 700°C show a broad band, like samples heated at lower temperatures, and Bragg peaks characteristic of crystalline YIG, consistent with the crystallization of the amorphous garnet phase.

The crystallite sizes were calculated from the XRD line broadening of the peak (420) using the classical Scherrer

TABLE 2
Series A Samples Treated for 2 and 12 h

Sample	Annealing temperature (°C)	Time (h)
A1	400	2
A2	400	12
A3	600	2
A4	600	12
A5	700	2
A6	700	12
A7	800	2
A8	800	12
A9	900	2
A10	900	12
A11	1000	2
A12	1000	12

relationship (8), $D_{hkl} = k\lambda/B \cos \theta$, where D_{hkl} is the particle diameter in Å, k is a constant (shape factor) with a value of 0.9, B is the half maximum linewidth, and λ is the wavelength of the X rays. For similar annealing, the obtained size is always smaller for the samples prepared without ethylene glycol. For samples A, B, and C, prepared with different quantities of citric acid, it is observed that the larger the citric concentration, the larger the size. Figure 4 shows the variation of the mean size, D_{420} , with the annealing time and temperature.

TRANSMISSION ELECTRON MICROSCOPY

Thin specimens for transmission electron microscopy (TEM) were obtained by ultrasonically dispersing the particles in *n*-butanol and disposing drops of this suspension on a Cu grid covered with a holey carbon film. This study was performed with a JEOL-2010 electron microscope operating at 200 kV and equipped with a side-entry $\pm 30^\circ$ double tilt specimen holder. The EDX

TABLE 1
Composition of Initial Solutions Used in the Gel Preparation

Series	$\text{Fe}(\text{NO}_3)_3$ (mol)	$\text{Y}(\text{NO}_3)_3$ (mol)	Citric acid (mol)	Water (mL)	Ethylene glycol (mL)
A	0.01	0.006	0.1	50	0
B	0.01	0.006	0.05	50	0
C	0.01	0.006	0.15	50	0
D	0.01	0.006	0.1	50	42
E	0.01	0.006	0.1	50	21
F	0.01	0.006	0.1	50	15
G	0.01	0.006	0.1	50	10
H	0.01	0.006	0.1	50	4
I	0.01	0.006	0.1	50	2

TABLE 3
Crystallographic Data for the Different Phases

JCPDS PDF card no.	Compound	Name	Space group	Unit cell parameters (Å)
33-693	$\text{Y}_3\text{Fe}_5\text{O}_{12}$	Garnet	$Ia\bar{3}d$ (230)	$a = 12.3774$
33-664	$\alpha\text{-Fe}_2\text{O}_3$	Hematite	$R\bar{3}c$ (161)	Rhombohedral $a = 5.0356$ $c = 13.7489$
39-1489	YFeO_3	Orthoferrite	$Pnma$ (62)	$a = 5.5946$ $b = 7.6053$ $c = 5.2817$
19-929	Fe_3O_4	Magnetite	$Fd\bar{3}m$ (227)	$a = 8.396$
39-1346	$\gamma\text{-Fe}_2\text{O}_3$	Maghemite	$P4_132$ (213)	$a = 8.3515$

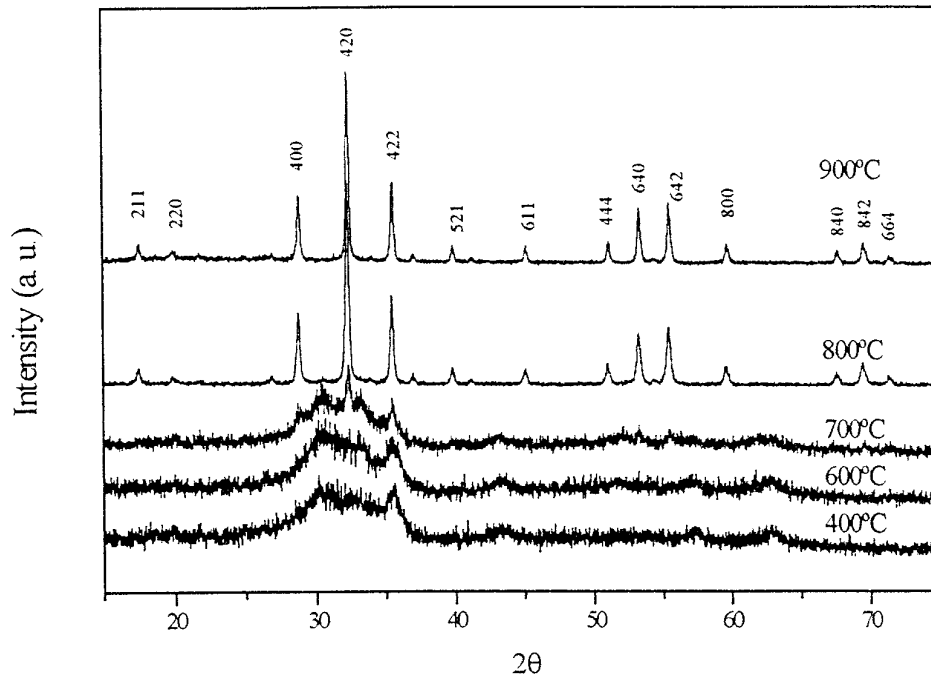


FIG. 2. XRD patterns of the A samples annealed 2 h (A1, A3, A5, A7, and A9).

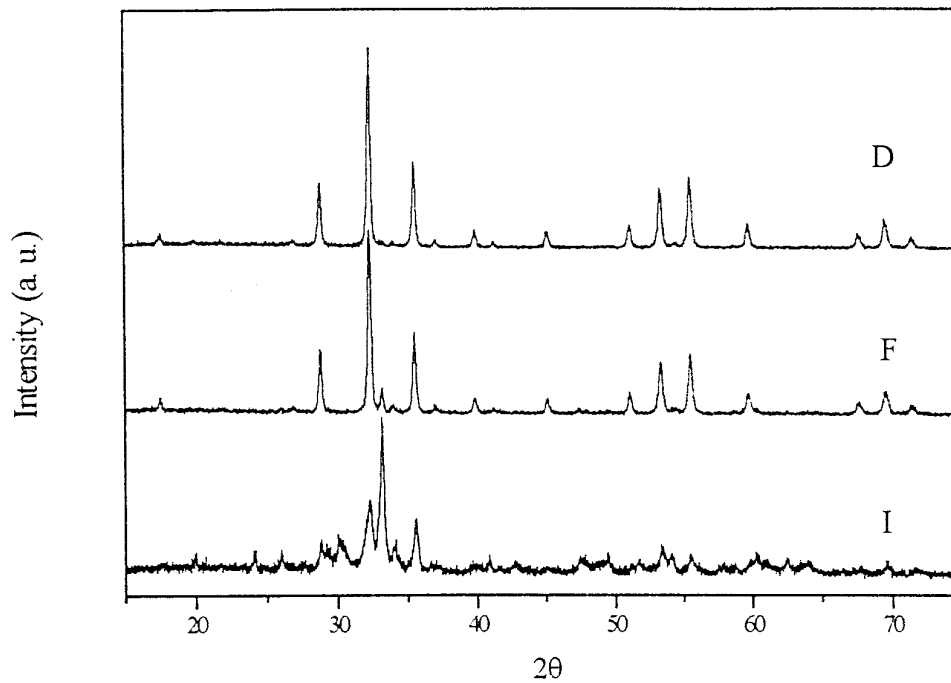


FIG. 3. XRD patterns of samples annealed at 800°C and prepared with different quantities of ethylene glycol (2, 15, and 42 mL, respectively).

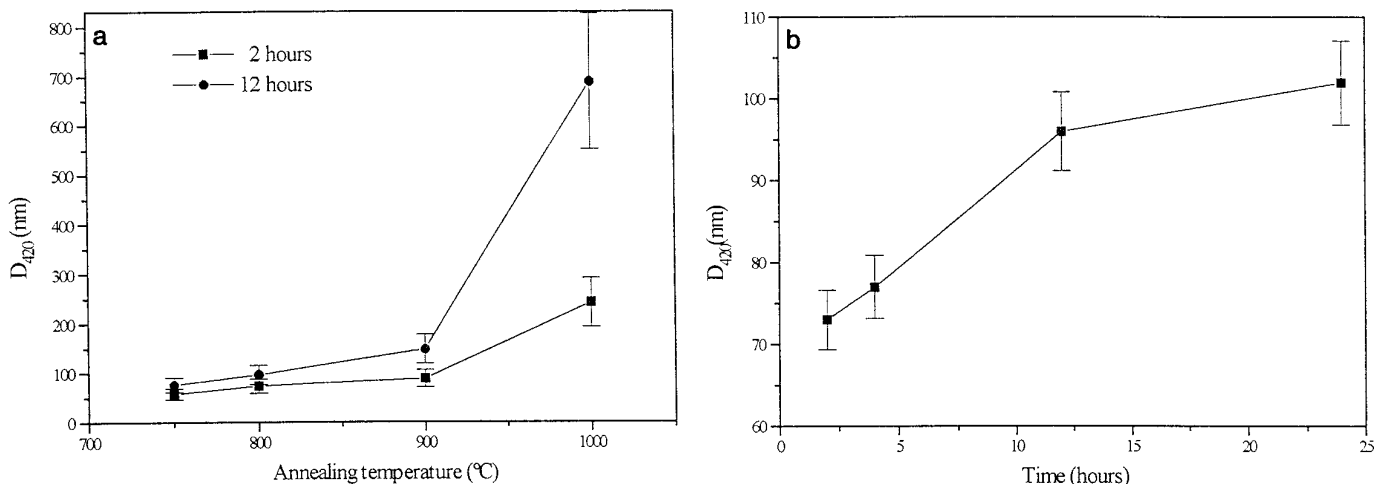


FIG. 4. (a) Mean size for the A samples heated at different temperatures. (b) Mean size for the A samples heated at 800°C for different times.

analysis was done with a KEVEX energy-dispersive X-ray spectrometer coupled with the TEM and allowed to approximate the composition of very small particles. TEM was used to study the composition, shape, size, size distribution, and crystallinity of the particles. This study was carried out on A samples.

The EDX study of a great number of particles confirms the presence of O, Fe, and Y and the homogeneity of the samples. No other phase was detected. An atomic ratio Y/Fe ≈ 0.7 was found, which is not very far from the

theoretical value (0.6), taking into account the accuracy of this method.

In all the samples, particles are aggregated (see Fig. 5) and exhibit rounded irregular shapes (without faceted borders), generally lengthened. An example of a typical particle is shown in Fig. 6, which reveals a detail of the surface morphology.

Table 4 shows the approximate mean sizes for the studied samples. Due to the aggregation of the particles and their irregular shapes, it is not possible to obtain more

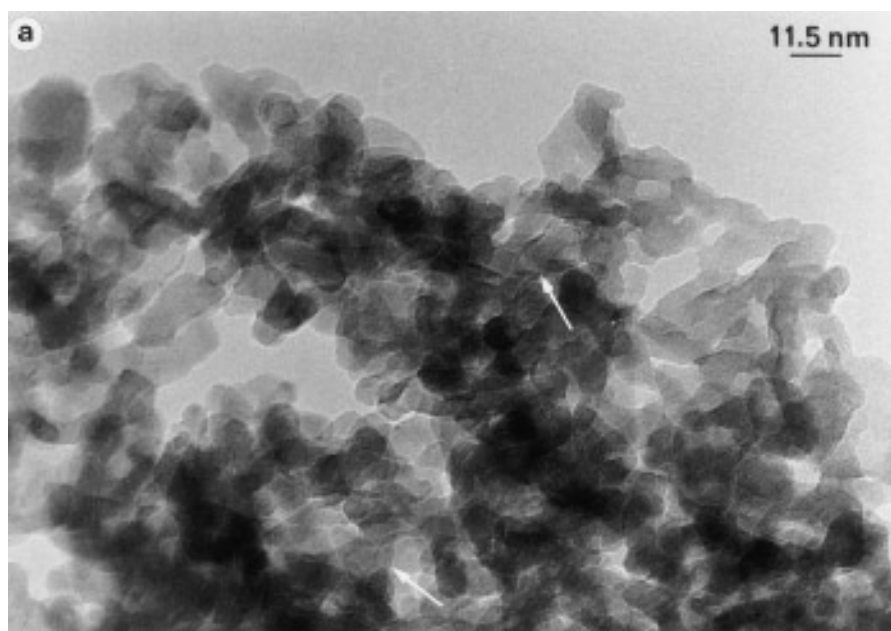


FIG. 5. Low-resolution images showing the morphology and the size distribution of particles of YIG samples after various temperatures of preparation: (a) 600°C (A4), (b) 800°C (A7), and (c) 1000°C (A12) (white arrows show the lattice fringes crystallization under the beam).

accurate values. One can observe, first, that size increases with the temperature of treatment of the samples (Fig. 5) and, second, that the sizes of the particles are similar to those calculated from XRD patterns.

The crystallinity of the samples increased with the temperature of treatment. During the study of the sample treated at 600°C (A4), crystallization of particles with beam heating occurred (see Fig. 7 and Fig. 5a): after a few

minutes of irradiation, the broad diffuse rings were transformed into rings with sharp spots as a result of crystallization due to the elevation of temperature of the imaged region.

Electron diffraction (ED) study, carried out on the sample treated at 1000°C (best crystallinity and largest particles), confirms the unit cell to be cubic with $a \approx 12.4 \text{ \AA}$. ED patterns of the [100] and [110] orientations are shown

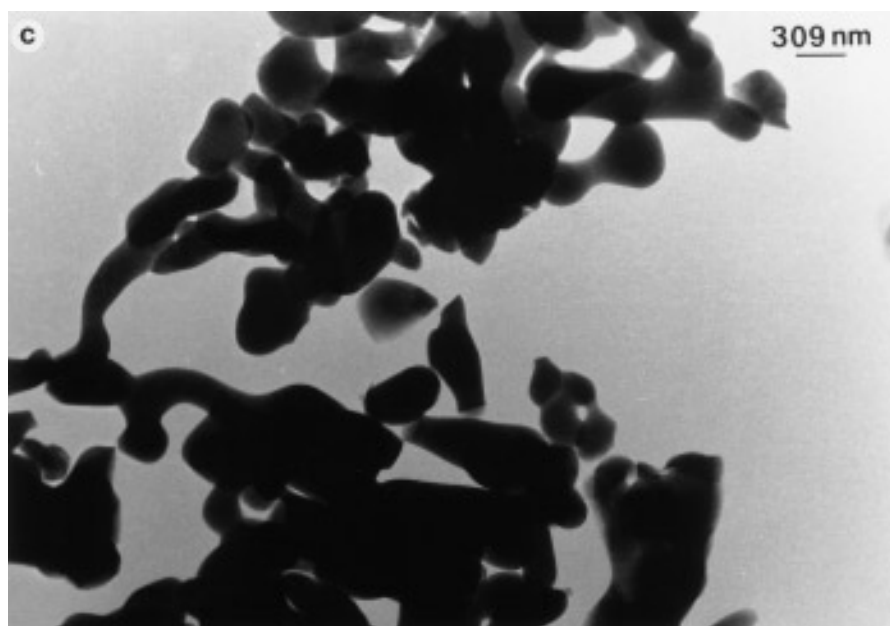
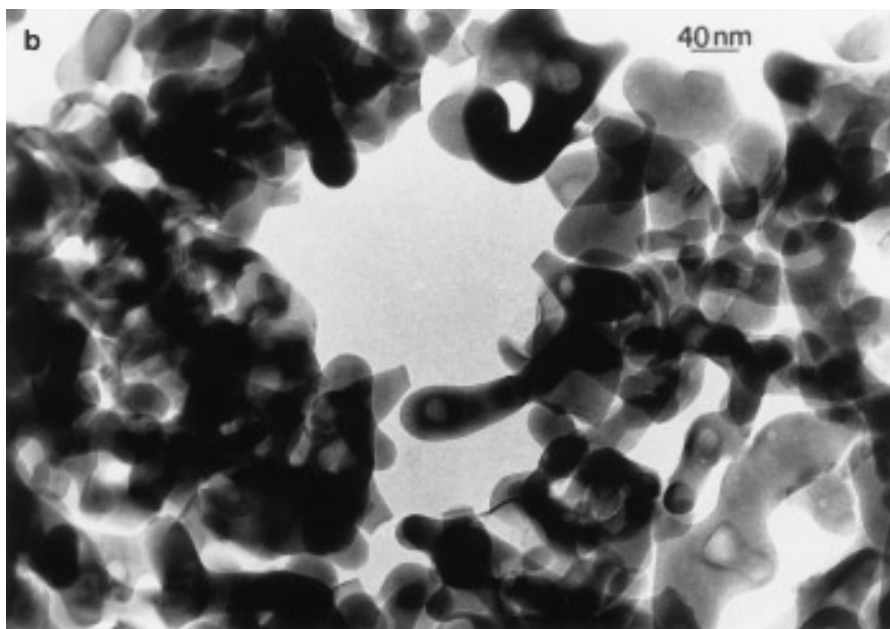


FIG. 5—Continued

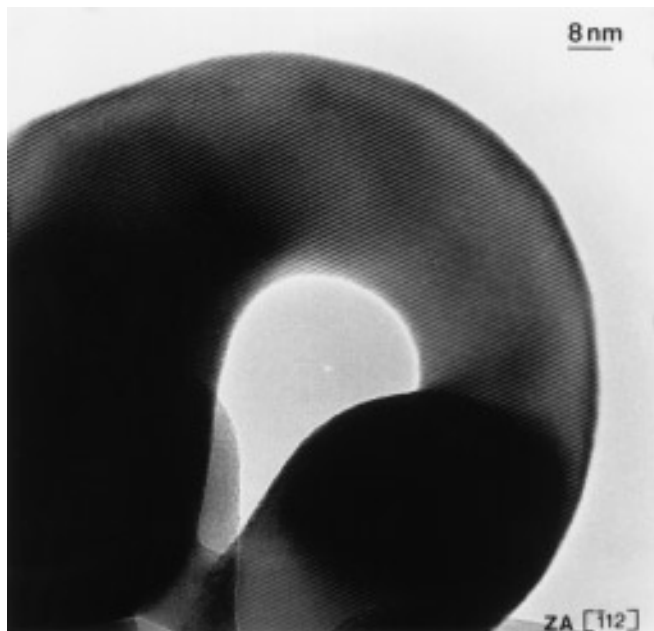


FIG. 6. HREM image along the $\bar{1}12$ zone axis showing a typical particle (treated at 800°C) with a rounded surface morphology (no faceted borders).

TABLE 4
Mean TEM Sizes for Different Samples

Sample	Mean TEM size (nm)
A4	20
A6	50
A7	100
A12	500

in Fig. 8. The weak reflections along the $[001]^*$ and $[0k0]^*$ reciprocal rows, which appeared at extinct positions on the ED corresponding to the $[100]$ zone axis, arose from double diffraction: their intensities were strongly affected by the rotation of the crystal along these directions. The scan of reciprocal space allowed the deduction of the extinction symbol $Ia\bar{d}$, compatible only with the space group $Ia\bar{3}d$ (230). These results are in good agreement with those expected.

Figure 9 shows a typical HREM image of the YIG viewed down the $\langle 100 \rangle$ direction, thus confirming the good crystallinity of the sample. One can remark the regular contrast observed, showing the absence of defects (stacking faults, dislocations, twinings) and the absence of amorphous phase at the edge of the particle. The simulated image has been calculated by the multislice method (slice

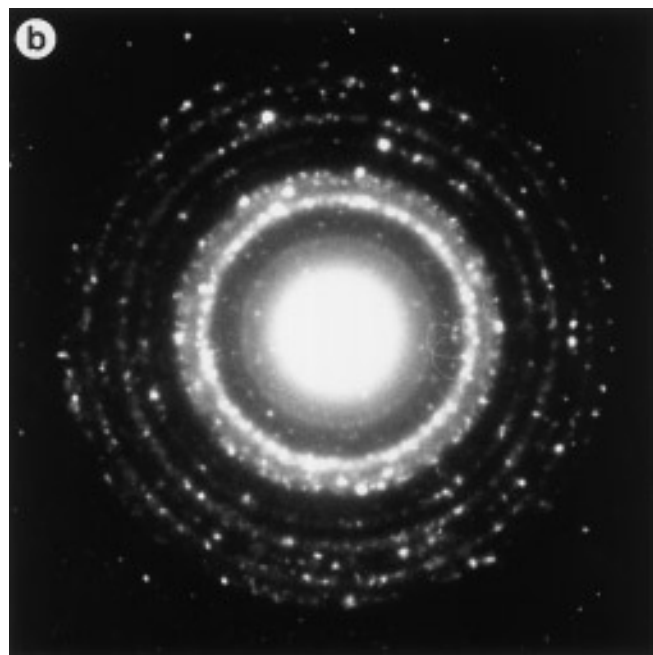
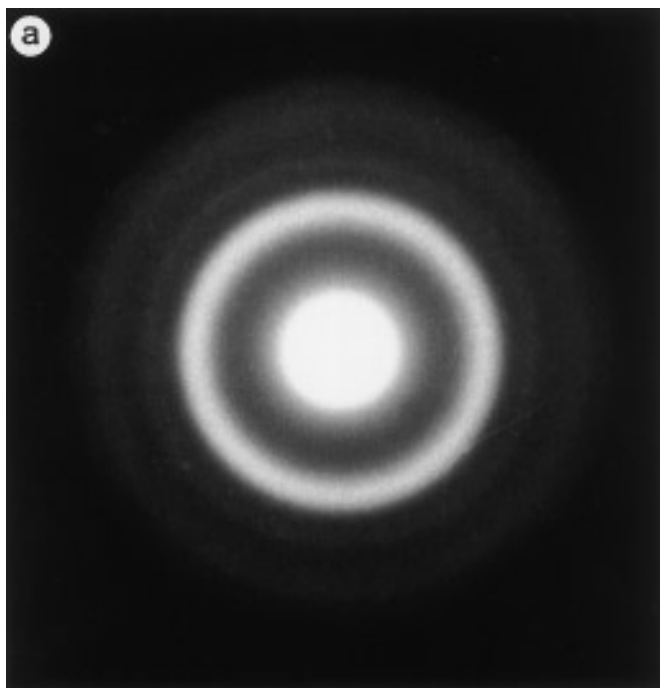


FIG. 7. Selected area diffraction pattern of a great number of particles treated at 600°C (A4). (a) Just after the area was chosen. (b) After a few minutes of irradiation, some spots appeared in the broad rings, indicating a crystallization process induced by the electron beam.

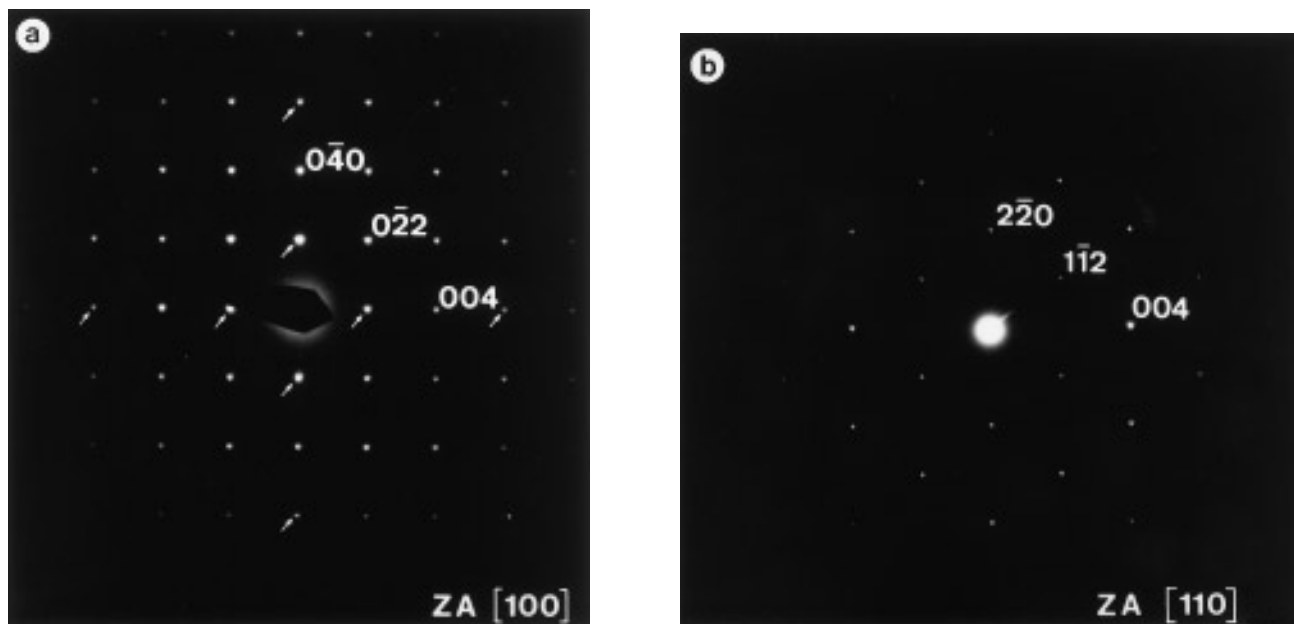


FIG. 8. Two sections of the reciprocal space of YIG: (a) [100] zone axis, (b) [110] zone axis (small white arrows show reflections arising from double diffraction).

thickness 1.768 \AA , sampling 128×128) with the EMS programs of Stadelman (9) using the following microscope parameters:

- acceleration voltage: 200 kV
- spherical aberration constant: $C_s = 1.0 \text{ mm}$

- defocus spread: $\Delta = 12 \text{ nm}$
- semi-convergence angle: $\alpha = 0.8 \text{ mrad}$
- objective lens aperture diameter: 11.6 nm^{-1} .

The cell parameters and the atomic coordinates of the atoms are taken from the YIG standard (10). One can

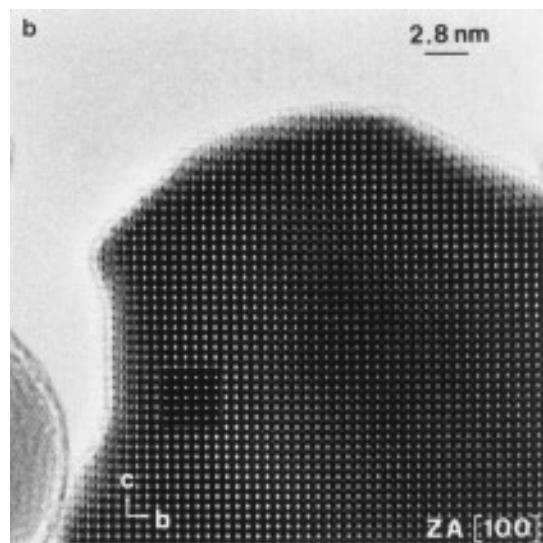
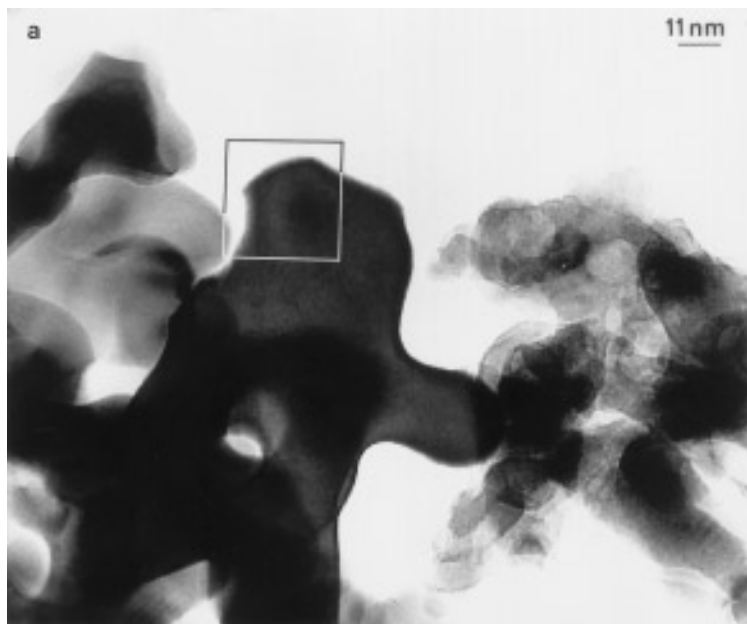


FIG. 9. HREM image of a YIG microcrystal along (100) zone axis showing the good crystallinity of this particle and the absence of defects. A detail of the observed image with the corresponding simulation for a specimen thickness of 37 \AA and a defocus value of 70 nm is given in (b).

see the good agreement between the simulated and the observed images.

CONCLUSIONS

Ultrafine YIG particles were synthesized by decomposition of a citrate gel. YIG is obtained above 700°C, a temperature lower than the 1300°C required in the ceramic method. The quality of samples prepared without ethylene glycol is better than the quality of the others. The particles obtained have a mean size smaller than those prepared with conventional methods. The particles have irregular rounded shapes, quite different from particles prepared by other methods. Particles present neither faceted borders nor amorphous phase at the edge, and defects are not observed.

ACKNOWLEDGMENT

P.V. acknowledges Xunta de Galicia for its financial support.

REFERENCES

1. R. J. Young, T. B. Wu, and I. N. Lin, *J. Mater. Sci.* **25**, 3566 (1990).
2. P. Apte, H. Burke, and H. Pickup, *J. Mater. Res.* **7**, 706 (1992).
3. O. Yamaguchi, K. Takeoka, K. Hirota, H. Takano, and A. Hayashida, *J. Mater. Sci.* **27**, 1261 (1992).
4. D. Roy, R. Bhatnagar, and D. Bahadur, *J. Mater. Sci.* **20**, 157 (1985).
5. V. K. Sankaranarayanan and N. S. Gajbhiye, *J. Am. Ceram. Soc.* **73**, 1301 (1990).
6. K. Matsumoto, K. Yamaguchi, and T. Fujii, *J. Appl. Phys.* **69**, 5918 (1991).
7. Joint Committee on Powder Diffraction Standard.
8. "International Tables for X-Ray Crystallography," Vol. III, 1985.
9. P. A. Stadelman, *Ultramicroscopy* **21**, 131 (1987).
10. S. Geller and M. A. Gilleo, *J. Phys. Chem. Solids* **9**, 235 (1959).